Chapter 4

Orthotopic mouse model for chondrosarcoma of bone: an *in vivo* tool for drug testing

This chapter is based on the manuscript: van Oosterwijk JG, Plass JRM, Meijer D, Que I, Karperien M, Bovée JVMG. Orthotopic mouse model for chondrosarcoma of bone: an *in vivo* tool for drug testing. *Submitted*

Abstract

Chondrosarcoma is a malignant cartilaginous tumor of bone. Recently, mutations in isocitrate dehydrogenase-1 (IDH1) and -2 (IDH2) were identified in central chondrosarcomas. Notoriously resistant to conventional treatment modalities the need for model systems to screen new treatment options is high.
We used two cell lines, CH2879 (wildtype for IDH and TP53 mutations) and SW1353 (harboring IDH2 R172S and TP53 V203L mutations) to generate new chondrosarcoma mouse models. Cell lines were stably transduced with a lentiviral luciferase expression vector and after clonal selection luciferase expressing clones were subcutaneously and orthotopically implanted in nude mice. Mice injected with CH2879 cells were treated with doxorubicin over a period of 6 weeks.
Both cell lines resulted in tumor growth. CH2879 tumors were consistently larger than SW1353 tumors. No difference in size could be observed between subcutaneous and orthotopic tumors. Tumor growth could be monitored over time through assessment of luciferase activity, without harming the mice. Using this model we show that doxorubicin does not have a significant effect on *in vivo* tumor growth.
We here show an orthotopic chondrosarcoma mouse model that can be used to test new treatment strategies evolving from *in vitro* research.

Introduction

Chondrosarcoma is a malignant cartilaginous tumor, predominantly affecting adults. Several subtypes with different clinicopathological features are recognized, of which conventional central chondrosarcoma is most common (~90%). Chondrosarcoma is characterized by the deposition of cartilaginous matrix, which is abundant in low grade tumors, and becomes more myxoid in high grade chondrosarcomas. Grade I chondrosarcoma has recently been reclassified as atypical cartilaginous tumor, due to its locally aggressive, but non-metastatic behavior (1). Grade II and grade III chondrosarcomas, showing a decrease in deposition of hyaline cartilaginous matrix along with increased cellularity, show an increased metastatic behavior (2). The current therapeutic strategy for chondrosarcoma is surgical resection, however due to the intrinsic resistance to conventional chemo- and radiotherapy there is nothing to offer patients with inoperable tumors and metastatic disease (3). The past decade has brought major advances in the field of chondrosarcoma genetics and therapeutic targets. Early on, EXT mutations have been identified in osteochondromas (4;5), and recently IDH mutations were identified in enchondroma, conventional central chondrosarcoma as well as dedifferentiated chondrosarcoma (6-8). The advances in the field also include an expansion in the number of cell lines. At the moment of writing there is a total of 7 conventional chondrosarcoma cell lines (9-13), and 3 dedifferentiated

chondrosarcoma cell lines (9;14). 5 of these cell lines show mutations in IDH1 (n=3) or IDH2 (n=2) (8;9). However, for advancing chondrosarcoma research and to rapidly translate results from basic research to clinical practice, reliable and representative animal models are necessary.
Most current models are based on the subcutaneous xenografting of chondrosarcoma cell lines or human tumor tissue, misrepresenting the natural niche of the tumor in the bone (15). Currently, a swarm rat chondrosarcoma model exists, derived from a tumor tissue line originally isolated from a spontaneously arising tumor in a Sprague-Dawley rat. Though a working model, the original tissue has given rise to several different lines of differentiation, each showing unique cytogenetic profiles and tumorigenic properties *in vivo* (16). In 2010, an orthotopic chondrosarcoma mouse model derived from the grade II cell line JJ012 was published. Cells were injected in matrigel, and 2/4 intratibial tumors showed spontaneous metastasis formation (17). Transgenic models for chondrosarcoma have not been developed yet. Mouse models with EXT mutations show formation of exostoses, but no progression to chondrosarcoma (18-20). Similarly, transgenic mice carrying IDH mutations in neural progenitor cells show a defect in collagen maturation, but no chondrosarcoma formation (21).
We here present 2 models, derived from the grade II SW1353 (IDH2 R172S p53 V203L) cell line and from the grade III CH2879 (IDH wt p53 wt) cell line. Using CH2879 we were able to confirm the resistance to doxorubicin, and show that this model can be used for pre-clinical therapeutic testing.

Methods

Cell lines
The chondrosarcoma cell lines CH2879 and SW1353 were cultured in RPMI 1640 medium (Invitrogen) supplemented with 10% heat-inactivated fetal bovine serum (Lonza, Breda, the Netherlands), 1% glutaMAX (Invitrogen, Bleiswijk, the Netherlands), and 50 U/mL penicillin with 50 µg/mL streptomycin (MP Biomedicals, Eindhoven, the Netherlands). Hek293t cells were cultured in DMEM (Invitrogen, Bleiswijk, the Netherlands) supplemented with 10% heat-inactivated fetal bovine serum (Lonza) and 100 U/mL penicillin with 100 µg/mL streptomycin.

Production of lentiviral particles in Hek293t cells
The self-inactivating lentiviral vector, pLV.CMV.luc.bc.PURO, and "helper" vectors, pMD 2\VSV-G, pMD L\pRRE, and pRSV-rev, were kindly provided by dr. Eric Kaijzel (LUMC). Briefly, the lentiviral vector together with the three "helper" vectors were cotransfected overnight into Hek293t cells using Lipofectamine 2000 (Invitrogen, Bleiswijk, the Netherlands) in OptiMem (Invitrogen, Bleiswijk, the Netherlands) after which medium was replaced by fresh culture medium. Viral supernatants were harvested 48hrs after transfection, filtered

through a 0.45 μm filter, and stored at -80°C until transduction in chondrosarcoma cell lines.

Generation of clonal luciferase expressing chondrosarcoma cell lines
The chondrosarcoma cells were transduced with the lentiviral supernatant in the presence of 1 μg/mL dextran (Sigma-Aldrich, Zwijndrecht, the Netherlands) for 4 hours. After transduction, cells were selected using 2 μg/mL puromycin (Sigma-Aldrich, Zwijndrecht, the Netherlands). Following antibiotic selection, single cell-derived cultures were obtained using limited dilution and screened for luciferase activity. As estrogen signaling was shown to be active in cartilaginous tumors (22), clones were selected using TaqMan gene expression arrays for ESR1, CYP19A1, and AR according to manufacturer's protocol (Applied Biosystems, Bleiswijk, the Netherlands). All cultures selected for *in vivo* implantation were tested for the presence of HIV p24.

Animals
All procedures were approved by the Leiden University animal experimental committee and Local Government (Animal protocols 08158 and 10019), performed in accordance with the national legislation of the Netherlands and in compliance with the 'Code of Practice Use of Laboratory Animals in Cancer Research' (Inspectie W&V, July 1999). Athymic mice (BALB/c *nu/nu* 6 weeks old) were acquired from Charles River (Charles River, L'Arbresle, France), housed in individually ventilated cages, and food and water was provided *ad libitum*. For all *in vivo* experiments, a total of 46 mice were used.

CH2879 and SW1353 tumor cell injection in mice
For both CH2879 and SW1353 cell lines, three single-cell derived luciferase expressing clones were used for both subcutaneous and orthotopic implantation into mice. 12 mice were subcutaneously injected. A total of 4 mice were injected with the different CH2879 clones, 4 mice with the different SW1353 clones and 4 with non-transduced cell lines to control for interference with tumorigenicity by luciferase construct.
Orthotopic injection was performed using two separate methods. In total 33 mice were orthotopically injected with either SW1353 or CH2879. Mice were anesthetized by isoflurane prior to subcutaneous or orthotopic injection in the tibia with luciferase expressing cells ($1*10^6$ cells in 40 μL PBS or $2.5*10^5$ cells in 10 μL PBS respectively). Eighteen mice were injected using the first method; 9 with SW1353 LUC clones and 9 with CH2879 clones; 3 mice per clone. Orthotopical injection was performed with an injection of a single-cell suspension of luc+ cells into the right tibiae as described previously (23). In brief, two small holes (~0.35mm each) 4-5 mm apart were created in the bone cortex of the upper right tibiae using a dental drill, and reservoir for the cells was created by flushing out the bone marrow from the proximal end of the shaft. After inoculation with a 30-gauge

needle through the lower hole, the cutaneous wound was sutured. In the second method, 15 mice were injected with CH2879 LUC 10. Orthotopical injection was performed with an injection of a single cell suspension directly into the tibia without the prior creation of a reservoir.
The progression of cancer cell growth was monitored weekly by optical imaging. After the experimental period, or 7 weeks after start of signal detection for mice not on treatment regime, the animals were sacrificed and tumors were collected for histological assessment.

In vivo treatment of CH2879 orthotopic tumors
The 15 mice injected using the second method (immediate injection without prior creation of a reservoir), were divided into two groups after signal detection for investigating the effect of doxorubicin on tumor growth. Seven mice were treated with 12 mg/kg doxorubicin over a course of 6 weeks in which they were administered a single dose once every 2 weeks through i.p. injection. Control group consisted of eight mice monitored over 6 weeks. Doxorubicin was obtained from the in-house hospital pharmacy in a 0.9% NaCl solution. Treatment was started when tumors could be detected using the IVIS 100 (Caliper LifeSciences, Hopkinton, MA), ie bioluminescent (BLI) signals of 10^5 P/s/cm^2 (~0.6cm^3). In case mice would show a bioluminescent signal $\geq 10^9$ P/s/cm^2 (~1cm^3) they were to be considered to have too severe a tumor burden and were sacrificed. After treatment course was completed, or mice showed severe clinical signs as a result of tumor burden or treatment, mice were sacrificed and tibiae were collected for histological assessment. Lungs were harvested to investigate possible metastases.

In vivo imaging
To monitor luciferase activity, mice were anesthetized using isoflurane. Images were acquired 5 minutes after i.p. injection of D-luciferin (150 mg/kg) using 30 sec exposure time. Tumor take was monitored using the IVIS 100 (Caliper LifeSciences, Hopkinton, MA) and bioluminescent signals were quantified using Living Image 3.0 (Caliper LifeSciences, Hopkinton, MA).

Tissue embedding and staining
Lungs were fixed in 4% paraformaldehyde and embedded in paraffin. Tibiae were decalcified in 0.4M EDTA/PBS after fixing in 4% paraformaldehyde. After decalcification with EDTA, tibiae were embedded in paraffin and 5µm sections were stained with hematoxylin and eosin (H&E) for morphology or 0.08% toluidine blue (Brocacef Holding, Maarssen, The Netherlands) to assess matrix formation.

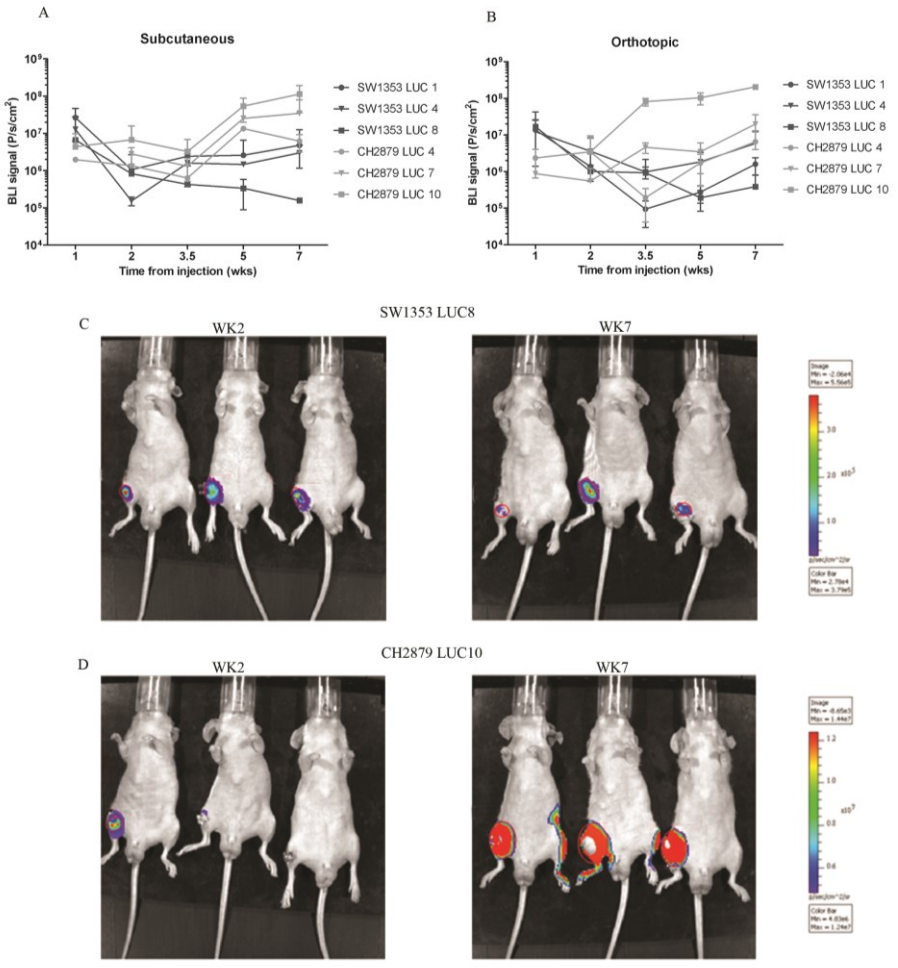

Figure 4.1: Generation of chondrosarcoma mouse model. A: Subcutaneous injection of SW1353 and CH2879 cells led to tumor growth in 4/4 mice. Standard deviation indicates variation in measurements between the 4 injected mice. B: Orthotopic injection of SW1353 and CH2879 cells led to tumor growth in 3/3 mice, CH2879 clone luc 10 resulted in larger tumors than other clones. Standard deviation indicates variation in measurements between the 4 injected mice. C: Each SW1353 clone was injected orthotopically in the left tibia of 3 mice. SW1353 clone 8 is shown with BLI signals at week 2 (left panel) and week 7 (central panel) with luminescence scale (right panel). Luciferase signals for this clone did not show an increase during the 7 week observation time. Standard deviation indicates variation in measurements between the 9 injected mice. D: Each CH2879 clone was injected orthotopically in the left tibia of 3 mice. CH2879 clone LUC 10 is shown with BLI signals at week 2 (left panel) and week 7 (central panel) with luminescence scale (right panel). This clone showed the strongest increase in luciferase signals during the 7 week observation time, as evidenced by the strong red signal. Standard deviation indicates variation in measurements between the 9 injected mice.

Results

Transduction of CH2879 and SW1353 cell lines

Based upon expression of estrogen signaling markers (results not shown), three representative clones were selected for each cell line. For SW1353, clones 1, 4, and 8 most closely resembled the nontransduced cell line, for CH2879, clones 4, 7, and 10 were most similar. All clones showed luciferase expression and were negative for HIV p24.

Tumor growth after injection of luciferase transduced SW1353 and CH2879 chondrosarcoma cell lines

Six week old Balb/C nude mice were injected with either SW1353 or CH2879. Tumor growth was observed within 1 week, evidenced by emission of bioluminescent signal at the first measurement (week 1) after both subcutaneous (fig 4.1A) and orthotopic (fig 4.1B, C, D) injection. Subcutaneous injection of SW1353 clone 1 and 4 led to tumors in 4/4 mice, whereas clone 8 led to tumors in 1/4 mice, orthotopic injection of SW1353 clones led to tumor growth in all cases (9/9 mice). CH2879 clone 4 and 7 led to tumor growth in 3/4 mice, clone 4 led to tumor growth in 4/4 mice, orthotopic injection of CH2879 clones led to tumor growth in all 9 mice. No bioluminescent signals were observed in the lungs and histological examination also indicated no evidence of metastases.

Luciferase activity of CH2879 tumors continued to increase during the course of 7 weeks, indicative of progressive tumor growth, whereas SW1353 derived tumors showed a stagnated signal strength, suggestive of halted growth. The size of the CH2879 derived tumors were consistently larger than the SW1353 derived tumor, as evidenced by stronger BLI signals (fig 4.1A, B). In both SW1353 and CH2879, orthotopic and subcutaneous injection resulted in comparable BLI signal. The clone showing the strongest luciferase signal, CH2879 LUC 10, (fig 4.1B, D), was selected for further experiments. Orthotopic injection of luciferase transfected cells using prior creation of a reservoir for the cells led to tumor growth within one to two weeks. Using the second method using immediate injection of the cells, it took up to 4 weeks until tumors were detectable by bioluminescent imaging. However, as immediate orthotopic injection was considered less painful for the mice and did result in successful tumor growth, in subsequent experiments mice were directly injected with tumor cells.

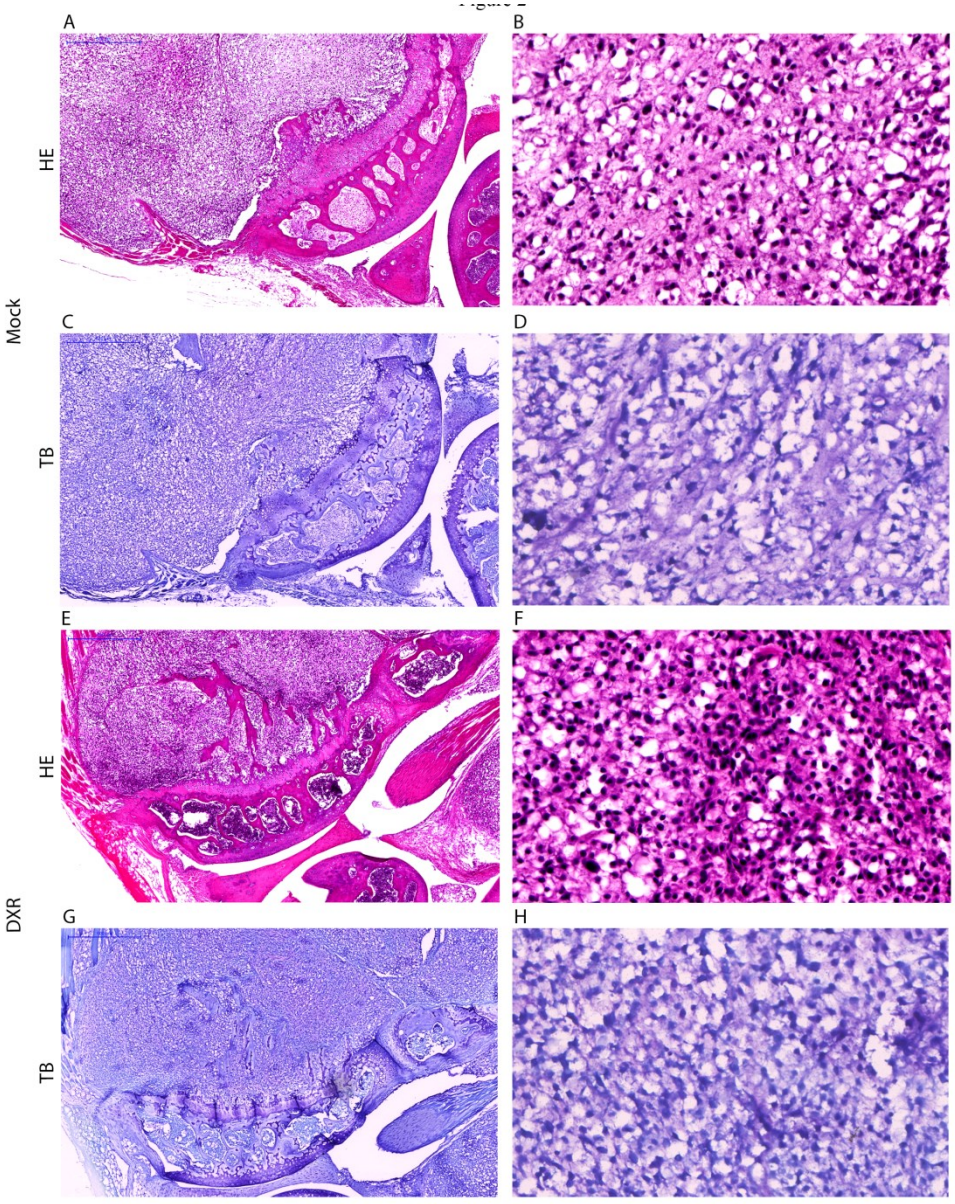

Figure 4.2: Orthotopic CH2879 tumor resemble chondrosarcoma morphology with matrix deposition. Control mouse (Mock A-D) and mouse treated with doxorubicin (DXR, E-H) using H&E staining (A,B; E,F) and toluidine blue staining (C,D; G,H) showing purple coloration where cartilaginous matrix is produced.

CH2879 tumors resemble high grade chondrosarcoma
Orthotopic injection of CH2879 LUC 10 cells shows diaphyseal localization of tumor cells, with tumor cells growing circumferentially and expanding through the cortex (fig 4.2 A, E). The histological analysis of the tumor cells shows that they strongly resemble that of a high grade chondrosarcoma (fig 4.2 B, D, F, H). The tumor is located close to the growth plate, but does not infiltrate the growth plate (fig 4.2 A, C, E, G). Toluidine blue staining shows matrix formation (fig 4.2 C, D, G, H).

Doxorubicin treatment does not influence chondrosarcoma tumor growth
Mice orthotopically injected with CH2879 LUC 10 cells were treated with doxorubicin 12mg/kg for 6 weeks. Treatment started when luciferase measurements were at BLI 10^5. Mean BLI starting values for mice on doxorubicin (n=7) were $8.4x10^6$ P/s/cm^2 ($\pm 3.5\ x10^6$) with end BLI values $1.9x10^8$ P/s/cm^2 ($\pm 1.5\ x10^8$). For the control group (n=8) starting BLI values were $4.1x10^6$ P/s/cm^2 ($\pm 5.3\ x10^6$) with end BLI values $5.9x10^7$ P/s/cm^2 ($\pm 2.1\ x10^7$). Fold change of tumor growth at the start of treatment was set at 1 to allow for comparison of the different groups. After start of treatment, mice receiving doxorubicin showed a delay in tumor progression when compared to control mice (fig 4.3A). However, during the last cycle of doxorubicin, a strong increase in tumor growth was observed (fig 4.3A), suggesting resistance to doxorubicin. Figure 4.3 B-E shows bioluminescent imaging of 3 control mice at start of treatment (fig 4.3B) and end of treatment (fig 3C) as well as 3 mice treated with doxorubicin at start of treatment (fig 4.3D) and end of treatment cycle (fig 3E) along with the luminescence scale (fig 4.3F). As tumors in the doxorubicin treated group show stronger BLI signals both at start and end of treatment, the total tumor growth over the course of 6 weeks, as calculated by fold change (fig 4.3A), amounts to a similar signal increase. Statistical analysis of both the BLI signals and the fold change showed that doxorubicin treatment was not found to significantly influence the tumor growth (two tailed independent t-test for fold change $p=0.143$; for BLI signals $p=0.2$). Mouse weight was stable during the entire experiment.

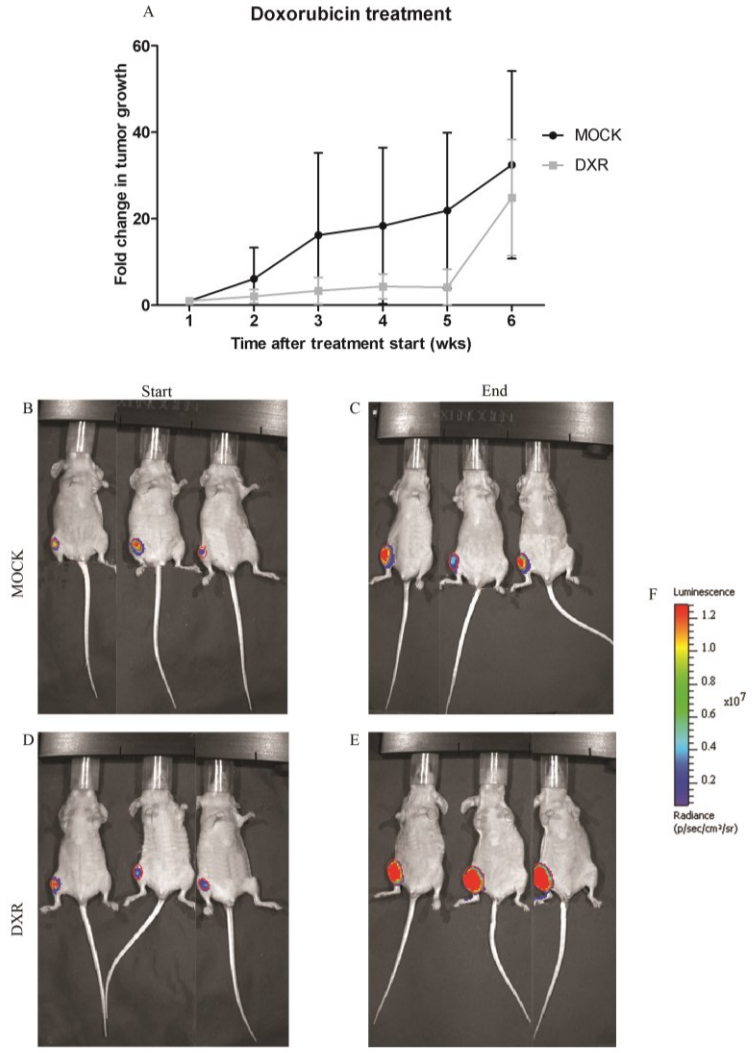

Figure 4.3: Orthotopic CH2879 tumors are resistant to doxorubicin. A: Mice were followed for bioluminescent signal indicating tumor presence from injection of tumor cells. At treatment start fold change of tumor growth was set at 1 and change in tumor growth monitored per week. Treated mice (DXR) showed a short lapse in tumor growth but start to catch up with untreated (MOCK) mice in tumor size at week 6. Standard deviation indicated variation in measurements of 8 untreated mice, and 7 doxorubicin treated mice. B,C: Bioluminescent signals for 3 untreated mice at start of signal detection (B) and after 6 weeks (C). D, E: Bioluminescent signals for 3 mice treated with doxorubicin at start of signal detection and doxorubicin treatment (D) and after 6 weeks at completion of treatment cycle (E). F: Luminescence scale indicating the strength of BLI signals in p/sec/cm^2/sr, based on the premise that a larger tumor will emit more luciferase and therefore a stronger signal will be detected, represented in the red spectrum on the scale. The increase is tumor size from B-C and D-E in control and doxorubicin treated mice is observed by the increase in red signal.

Discussion

Chondrosarcoma is notoriously resistant to conventional chemotherapy. The mouse model developed here supports this resistance as it is observed in the clinic. Indeed, no significant difference between untreated tumors and tumors treated with doxorubicin is observed. In this era of targeted therapeutics, identification of targets is crucial, and over the past years new therapeutic targets have been identified using the growing number of chondrosarcoma cell lines. Apoptotic pathways have been shown to be upregulated in chondrosarcoma, and inhibition of survivin (24) and the anti-apoptotic Bcl-2 family members (25-27) were shown to result in increased sensitivity to chemotherapeutics and radiotherapy (28). Moreover, survival pathways involving HIF1α (29-31), Src (32;33), PI3K (32;34), and the mTOR (35;36) pathways have been shown to play crucial roles in chondrosarcoma survival. The development of new targeted therapeutics targeting the apoptosis and survival pathways provides unlimited opportunities for combination treatments. Recently, synergy between PI3K and Bcl-2/Bcl-xl inhibition was shown in renal cell carcinoma cell lines (37), and both were shown to potentiate MEK inhibition in lung and pancreatic tumor models (38). Preclinical results in chondrosarcoma strongly advocate similar combinations in chondrosarcoma. However, due to the rarity of chondrosarcoma, the execution of large clinical trials is a major hurdle. The presence of good animal models, such as the one presented here, to test therapeutic candidates before proceeding to the clinic is therefore invaluable.

Most existing chondrosarcoma mouse models are subcutaneous (15), whereas human chondrosarcoma typically occurs either in the medulla of the bone or on the surface of the bone (1). A mouse model mimicking the human situation is preferable when studying chondrosarcoma characteristics and new therapeutic strategies, especially since matrix deposition around the tumor cells and tumor blood supply have been hypothesized to play a role in chemoresistance (33). The models presented here utilize a luciferase construct enabling the live imaging of tumor growth, an especially useful tool when studying drug response. Interestingly, during the development of our model, we observed that direct deposition of tumor cells in the bone resulted in better grafting than subcutaneous injection. Possibly through creating a niche which better resembles the natural environment of the tumor. We compared two injection methods, in the first method cells were injected after drilling a hole in the tibia, and in the second method cells were immediately injected in the tibia. Even though a short delay in tumor onset was observed, tumors succeeded to grow without prior creation of a reservoir, a method also considered to be less painful for the mice.

However, subcutaneous xenograft chondrosarcoma mouse models have advanced our understanding of EXT mutations and the hedgehog signaling in cartilage tumors (39). Recently, an orthotopic xenograft mouse model with spontaneous metastases, derived from the chondrosarcoma cell line JJ012, was developed. We

were unable to grow tumors using the JJ012 cell line (results not shown). This discrepancy could be explained by the fact that we did not use matrigel to facilitate injection and homing of the chondrosarcoma cells. However, the CH2879 and SW1353 cell lines did not need matrigel to form tumors.

We here show the development of orthotopic chondrosarcoma mouse models, using a luciferase construct for live imaging of tumor growth. Strongly resembling human chondrosarcoma, these models provide a new tool for *in vivo* studying of targeted therapeutics. Especially in chondrosarcoma, a rare malignancy making large randomized trials difficult to conduct, the development of such a mouse model can aid in bridging the gap between pre-clinical research and clinical implementation of new therapeutic strategies.

Reference List

(1) Hogendoorn PCW, Bovée JVMG, Nielsen GP. Chondrosarcoma (grades I-III), including primary and secondary variants and periosteal chondrosarcoma. In: Fletcher C.D.M., Bridge JA, Hogendoorn PCW, Mertens F, editors. World Health Classification of Tumours. Pathology and Genetics of Tumours of Soft Tissue and Bone. 4 ed. 2013. p. 264-8.

(2) Evans HL, Ayala AG, Romsdahl MM. Prognostic factors in chondrosarcoma of bone. A clinicopathologic analysis with emphasis on histologic grading. Cancer 1977;40:818-31.

(3) Gelderblom H, Hogendoorn PCW, Dijkstra SD, van Rijswijk CS, Krol AD, Taminiau AH, Bovee JVMG. The clinical approach towards chondrosarcoma. Oncologist 2008;13(3):320-9.

(4) Jennes I, Pedrini E, Zuntini M, Mordenti M, Balkassmi S, Asteggiano CG, Casey B, Bakker B, Sangiorgi L, Wuyts W. Multiple osteochondromas: mutation update and description of the multiple osteochondromas mutation database (MOdb). Hum Mutat 2009;30(12):1620-7.

(5) Hecht JT, Hogue D, Strong LC, Hansen MF, Blanton SH, Wagner M. Hereditary multiple exostosis and chondrosarcoma: linkage to chromosome 11 and loss of heterozygosity for EXT-linked markers on chromosomes 11 and 8. Am J Hum Genet 1995;56:1125-31.

(6) Amary MF, Bacsi K, Maggiani F, Damato S, Halai D, Berisha F, Pollock R, O'Donnell P, Grigoriadis A, Diss T, Eskandarpour M, Presneau N, Hogendoorn PC, Futreal A, Tirabosco R, Flanagan AM. IDH1 and IDH2 mutations are frequent events in central chondrosarcoma and central and periosteal chondromas but not in other mesenchymal tumours. J Pathol 2011;224(3):334-43.

(7) Amary MF, Damato S, Halai D, Eskandarpour M, Berisha F, Bonar F, McCarthy S, Fantin VR, Straley KS, Lobo S, Aston W, Green CL, Gale RE, Tirabosco R, Futreal A, Campbell P, Presneau N, Flanagan AM. Ollier disease and Maffucci syndrome are caused by somatic mosaic mutations of IDH1 and IDH2. Nat Genet 2011.

(8) Pansuriya TC, van ER, d'Adamo P, van Ruler MA, Kuijjer ML, Oosting J, Cleton-Jansen AM, van Oosterwijk JG, Verbeke SL, Meijer D, van WT, Nord KH, Sangiorgi L, Toker B, Liegl-Atzwanger B, San-Julian M, Sciot R, Limaye N, Kindblom LG, Daugaard S, Godfraind C, Boon LM, Vikkula M, Kurek KC, Szuhai K et al. Somatic mosaic IDH1 and IDH2 mutations are associated with enchondroma and spindle cell hemangioma in Ollier disease and Maffucci syndrome. Nat Genet 2011;43(12):1256-61.

(9) van Oosterwijk JG, de JD, van Ruler MA, Hogendoorn PC, Dijkstra PS, van Rijswijk CS, Machado IS, Llombart-Bosch A, Szuhai K, Bovée JVMG. Three new chondrosarcoma cell lines: one grade III conventional central chondrosarcoma and two dedifferentiated chondrosarcomas of bone. BMC Cancer 2012;12(375):-375.

(10) Calabuig-Farinas S, Benso RG, Szuhai K, Machado I, Lopez-Guerrero JA, de JD, Peydro A, Miguel TS, Navarro L, Pellin A, Llombart-Bosch A. Characterization of a New Human Cell Line (CH-3573) Derived from a Grade II Chondrosarcoma with Matrix Production. Pathol Oncol Res 2012.

(11) Gil-Benso R, Lopez-Gines C, Lopez-Guerrero JA, Carda C, Callaghan RC, Navarro S, Ferrer J, Pellin A, Llombart-Bosch A. Establishment and characterization of a continuous human chondrosarcoma cell line, ch-2879:

comparative histologic and genetic studies with its tumor of origin. Lab Invest 2003;83(6):877-87.
(12) Scully SP, Berend KR, Toth A, Qi WN, Qi Z, Block JA. Marshall Urist Award. Interstitial collagenase gene expression correlates with in vitro invasion in human chondrosarcoma. Clin Orthop Relat Res 2000;(376):291-303.
(13) Kunisada T, Miyazaki M, Mihara K, Gao C, Kawai A, Inoue H, Namba M. A new human chondrosarcoma cell line (OUMS-27) that maintains chondrocytic differentiation. Int J Cancer 1998;77(6):854-9.
(14) Kudo N, Ogose A, Hotta T, Kawashima H, Gu W, Umezu H, Toyama T, Endo N. Establishment of novel human dedifferentiated chondrosarcoma cell line with osteoblastic differentiation. Virchows Arch 2007;451(3):691-9.
(15) Clark JC, Dass CR, Choong PF. Development of chondrosarcoma animal models for assessment of adjuvant therapy. ANZ J Surg 2009;79(5):327-36.
(16) Stevens JW, Patil SR, Jordan DK, Kimura JH, Morcuende JA. Cytogenetics of swarm rat chondrosarcoma. Iowa Orthop J 2005;25:135-40.
(17) Clark JC, Akiyama T, Dass CR, Choong PF. New clinically relevant, orthotopic mouse models of human chondrosarcoma with spontaneous metastasis. Cancer Cell Int 2010;10:20.
(18) Stickens D, Zak BM, Rougier N, Esko JD, Werb Z. Mice deficient in Ext2 lack heparan sulfate and develop exostoses. Development 2005 19;132(22):5055-68.
(19) Zak BM, Schuksz M, Koyama E, Mundy C, Wells DE, Yamaguchi Y, Pacifici M, Esko JD. Compound heterozygous loss of Ext1 and Ext2 is sufficient for formation of multiple exostoses in mouse ribs and long bones. Bone 2011 1;48(5):979-87.
(20) Matsumoto K, Irie F, Mackem S, Yamaguchi Y. A mouse model of chondrocyte-specific somatic mutation reveals a role for Ext1 loss of heterozygosity in multiple hereditary exostoses. Proc Natl Acad Sci U S A 2010;107(24):10932-7.
(21) Sasaki M, Knobbe CB, Itsumi M, Elia AJ, Harris IS, Chio II, Cairns RA, McCracken S, Wakeham A, Haight J, Ten AY, Snow B, Ueda T, Inoue S, Yamamoto K, Ko M, Rao A, Yen KE, Su SM, Mak TW. D-2-hydroxyglutarate produced by mutant IDH1 perturbs collagen maturation and basement membrane function. Genes Dev 2012;26(18):2038-49.
(22) Cleton-Jansen AM, van Beerendonk HM, Baelde HJ, Bovée JVMG, Karperien M, Hogendoorn PCW. Estrogen signaling is active in cartilaginous tumors: implications for antiestrogen therapy as treatment option of metastasized or irresectable chondrosarcoma. Clin Cancer Res 2005;11(22):8028-35.
(23) van der Pluijm G, Que I, Sijmons B, Buijs JT, Lowik CW, Wetterwald A, Thalmann GN, Papapoulos SE, Cecchini MG. Interference with the microenvironmental support impairs the de novo formation of bone metastases in vivo. Cancer Res 2005;65(17):7682-90.
(24) Lechler P, Renkawitz T, Campean V, Balakrishnan S, Tingart M, Grifka J, Schaumburger J. The antiapoptotic gene survivin is highly expressed in human chondrosarcoma and promotes drug resistance in chondrosarcoma cells in vitro. BMC Cancer 2011;11:-120.
(25) van Oosterwijk JG, Herpers B, Meijer D, Briaire-de Bruijn IH, Cleton-Jansen AM, Gelderblom H, van de Water B, Bovée JVMG. Restoration of chemosensitivity for doxorubicin and cisplatin in chondrosarcoma in vitro: BCL-2 family members cause

chemoresistance. Ann Oncol 2012;23(6):1617-26.
(26) van Oosterwijk JG, Meijer D, van Ruler MA, van den Akker BE, Oosting J, Krenacs T, Picci P, Flanagan AM, Liegl-Atzwanger B, Leithner A, Athanasou N, Daugaard S, Hogendoorn PCW, Bovee JVMG. Screening for Potential Targets for Therapy in Mesenchymal, Clear Cell, and Dedifferentiated Chondrosarcoma Reveals Bcl-2 Family Members and TGFbeta as Potential Targets. Am J Pathol 2013;182(4):1347-56.
(27) Kim DW, Kim KO, Shin MJ, Ha JH, Seo SW, Yang J, Lee FY. siRNA-based targeting of antiapoptotic genes can reverse chemoresistance in P-glycoprotein expressing chondrosarcoma cells. Mol Cancer 2009;8:28.
(28) Kim DW, Seo SW, Cho SK, Chang SS, Lee HW, Lee SE, Block JA, Hei TK, Lee FY. Targeting of cell survival genes using small interfering RNAs (siRNAs) enhances radiosensitivity of Grade II chondrosarcoma cells. J Orthop Res 2007;25(6):820-8.
(29) Boeuf S, Bovee JVMG, Lehner B, Hogendoorn PCW, Richter W. Correlation of hypoxic signalling to histological grade and outcome in cartilage tumours. Histopathology 2009.
(30) Chen C, Zhou H, Wei F, Jiang L, Liu X, Liu Z, Ma Q. Increased levels of hypoxia-inducible factor-1alpha are associated with Bcl-xL expression, tumor apoptosis, and clinical outcome in chondrosarcoma. J Orthop Res 2010.
(31) Schaap FG, French PJ, Bovee JVMG. Mutations in the Isocitrate Dehydrogenase Genes IDH1 and IDH2 in Tumors. Adv Anat Pathol 2013 January;20(1):32-8.
(32) Schrage YM, Briaire-de Bruijn IH, de Miranda NFCC, van Oosterwijk JG, Taminiau AHM, van Wezel T, Hogendoorn PCW, Bovée JVMG. Kinome profiling of chondrosarcoma reveals Src-pathway activity and dasatinib as option for treatment. Cancer Res 2009;69(15):6216-22.
(33) Bovee JVMG, Cleton-Jansen AM, Taminiau AHM, Hogendoorn PCW. Emerging pathways in the development of chondrosarcoma of bone and implications for targeted treatment. Lancet Oncology 2005 August;6(8):599-607.
(34) Galoian K, Temple HT, Galoyan A. mTORC1 inhibition and ECM-cell adhesion-independent drug resistance via PI3K-AKT and PI3K-RAS-MAPK feedback loops. Tumour Biol 2012 June;33(3):885-90.
(35) Perez J, Decouvelaere AV, Pointecouteau T, Pissaloux D, Michot JP, Besse A, Blay JY, Dutour A. Inhibition of chondrosarcoma growth by mTOR inhibitor in an in vivo syngeneic rat model. PLoS ONE 2012;7(6):e32458.
(36) Bernstein-Molho R, Kollender Y, Issakov J, Bickels J, Dadia S, Flusser G, Meller I, Sagi-Eisenberg R, Merimsky O. Clinical activity of mTOR inhibition in combination with cyclophosphamide in the treatment of recurrent unresectable chondrosarcomas. Cancer Chemother Pharmacol 2012;70(6):855-60.
(37) Zhu S, Cohen MB, Bjorge JD, Mier JW, Cho DC. PI3K inhibition potentiates Bcl-2-dependent apoptosis in renal carcinoma cells. J Cell Mol Med 2013;17(3):377-85.
(38) Tan N, Wong M, Nannini MA, Hong R, Lee LB, Price S, Williams K, Savy PP, Yue P, Sampath D, Settleman J, Fairbrother WJ, Belmont LD. Bcl-2/Bcl-xL Inhibition Increases the Efficacy of Mek Inhibition Alone and in Combination with PI3 Kinase Inhibition in Lung and Pancreatic Tumor Models. Mol Cancer Ther 2013.
(39) Tiet TD, Hopyan S, Nadesan P, Gokgoz N, Poon R, Lin AC, Yan T, Andrulis IL, Alman BA, Wunder JS.

Constitutive hedgehog signaling in chondrosarcoma up-regulates tumor cell proliferation. Am J Pathol 2006;168(1):321-30.